A Dinuclear Iron Complex Based on Parallel Malonate Binding Sites: Cooperative Activation of Dioxygen and Biomimetic Ligand Oxidation

Inke Siewert,[a] Christian Limberg,*[a] Serhiy Demeshko,[b] and Elke Hoppe[a]

Dedicated to Professor Helmut Schwarz on the occasion of his 65th birthday

Abstract: A ligand that offers two parallel malonate binding sites linked by a xanthene backbone, namely, Xanthmal^{2-}, has been utilised to synthesise dinuclear Fe^{II} complex [Fe$_2$-(Xanthmal)$_2$] (**1**). The reactivity of **1** in contact with O$_2$ was investigated at $-40\,°C$ and room temperature. After activation of O$_2$ through interaction with both iron centres the ligand is oxidised: at the C$_\alpha$ position monooxygenation and peroxide formation occur, partially accompanied by C$-$C bond cleavage to yield α-keto ester groups. To reveal mechanistic details investigations concerning 1) peroxide decomposition, 2) the reactivity of a corresponding mononuclear complex, 3) the influence of monooxygenation of the ligand on the reactivity and 4) product formation in dependence on time were carried out. The results can be explained by p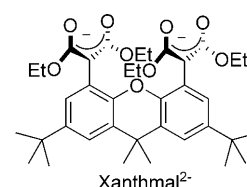ostulating formation of high-valent Fe intermediates and ligand-to-metal electron transfer, and the mechanistic scheme derived includes several steps that mimic the (suggested) functioning of non-heme iron enzymes. In agreement with this proposal, ligand oxidation can also be performed catalytically. Furthermore, we show that via a competitive route [(Xanthmal)$_2$Fe$_2$O] (**2**) is formed, which is unreactive towards O$_2$ and thus is a dead end with respect to ligand oxidation. Both compounds **1** and **2** were fully characterised, and their properties are discussed.

Keywords: iron · O ligands · O$-$O activation · oxygenation · reaction mechanisms

Introduction

Numerous examples in the literature show that the cooperation of metal centres in redox or hydrolytic reactions can lead to significant improvements,[1] and in fact this concept is also utilized in many metalloenzymes.[2] It therefore seems rewarding to develop ligands that are preorganised for complexation of two metal centres and thereby support their cooperation. In this context we have recently reported the ligand Xanthmal^{2-} with two adjacent diethyl malonate binding sites linked by a xanthene backbone,[3] which is utilised in the present study for the preparation of a dinuclear iron(II) complex. The question arose whether this ligand can support cooperation of two Fe^{II} centres for the activation of O$_2$ by analogy to the prosthetic group of soluble methane monooxygenase (sMMO).[4] A

Xanthmal^{2-}

further aspect of using malonate binding pockets is that they represent 2,4-pentadione derivates which serve as substrates for acetylacetone dioxygenase,[5] a non-heme enzyme that catalyses oxidative degradation of such units. Here we report on the results of this investigation, which indeed revealed biomimetic O$_2$ activation and ligand oxidation by complex mechanisms.

[a] I. Siewert, Prof. Dr. C. Limberg, Dr. E. Hoppe
Institut für Chemie
Humboldt-Universität zu Berlin
Brook-Taylor-Strasse 2, 10829 Berlin (Germany)
Fax: (+49) 30-2093-6966
E-mail: christian.limberg@chemie.hu-berlin.de

[b] Dr. S. Demeshko
Institut für Anorganische Chemie
Georg-August-Universität Göttingen
Tammannstrasse 4, 37077 Göttingen (Germany)

Supporting information for this article is available on the WWW under http://dx.doi.org/10.1002/chem.200800955.

Results and Discussion

Complex formation: Synthesis of an iron(II) complex of Xanthmal^{2-} was pursued by salt metathesis. After deprotonation of ligand precursor (Xanthmal)H$_2$ at the C$_\alpha$ position

by lithium diisopropylamide (LDA) in THF, the resulting lithium salt was isolated and purified.[3] After its re-dissolution, one equivalent of FeCl$_2$ or [Fe(OTf)$_2$(MeCN)$_2$] (OTf = trifluoromethanesulfonate) was added, and the resulting white precipitate was washed with THF. Characterisation of this product by IR spectroscopy, elemental analysis and single-crystal X-ray diffraction revealed it to be [Fe$_2$-(Xanthmal)$_2$] (**1**), which was isolated in good yields (Scheme 1).
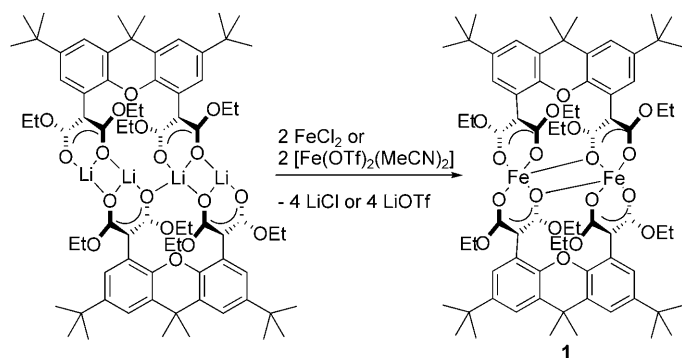
Scheme 1. Synthesis of [Fe$_2$(Xanthmal)$_2$] (**1**).

In **1** the two Fe^{II} ions are coordinated by two ligand equivalents, and it is formed independently of the molar ratio of the reactants employed. The molecular structure of **1** is shown in Figure 1.
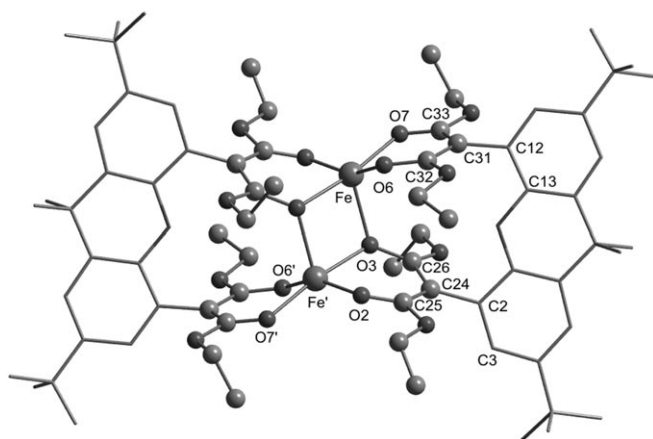

Figure 1. Molecular structure of **1**. All hydrogen atoms and one disordered, co-crystallised diethyl ether molecule are omitted for clarity. Selected bond lengths [Å] and angles [°]: Fe–Fe′ 3.281(2), Fe–O2 1.986(4), Fe–O3 2.089(3), Fe–O6 1.967(4), Fe1–O7 2.022(3), Fe′–O3 2.147(4); O6-Fe1-O7 85.6(2), O3-Fe1-O2 84.4(2).

The molecules exhibit a crystallographic centre of inversion, and the diethyl malonate moieties are twisted with respect to the xanthene backbone (C13-C12-C31-C33 65.0, C3-C2-C24-C25 65.0°). As indicated by the C–O bond lengths and the C-C-C angles of the individual malonate

binding pockets (e.g., C25-C24-C26 119.4°) the negative charge is delocalised over the malonate backbones. The iron ions are five-coordinate in a distorted square-pyramidal geometry with the Fe atoms displaced from the O$_4$ basal planes by 0.3 Å. The planes defined by the diethyl malonate units are somewhat tilted in a way that brings the two Fe atoms closer together, and the Fe–Fe distance of 3.281 Å is thus significantly shorter than that reported for dinuclear bis-β-diiminato iron complexes based on the xanthene backbone (4.239 Å)[6] or the Zn–Zn distance in [(Xanthmal)$_2$Zn$_2$] (3.766 Å).[3] Considering the non-bridging O atoms for each iron centre reveals two short Fe–O distances (O2, O6) and one which is slightly longer (O7). The bond lengths involving the bridging O atoms are longer. Complex **1** is EPR silent. Its magnetic moment μ_{eff} at 295 K amounts to 7.60 μ_B per complex, which is somewhat higher than the spin-only value expected for two uncoupled high-spin Fe^{II} ions (6.93 μ_B). Temperature-dependent measurement of the magnetic susceptibility shows weak ferromagnetic coupling: the effective magnetic moment increases below 50 K (Figure S1, Supporting Information).[7] Experimental data were modelled by fitting the appropriate Heisenberg–Dirac–van Vleck spin Hamiltonian for two $S = 2$ iron centres with isotropic exchange coupling, Zeemann splitting and zero-field splitting [Eq. (1)].[8]

$$\hat{H} = -2J\hat{S}_1\hat{S}_2 + g\mu_B(\hat{S}_1 + \hat{S}_2) + 2D[S_z^2 - 1/3S(S+1)] \qquad (1)$$

The best fit gave values of $g_1 = g_2 = 2.1$, $J = 0.3$ cm^{-1} and $|D| = 4.8$ cm^{-1} (the calculated curve fit is shown as a solid line in Figure S1, Supporting Information).[9] It should be pointed out that the fully reduced form of sMMO also exhibits a weak ferromagnetic exchange coupling at lower temperatures ($J = 0.3–0.5$ cm^{-1}).[10] A Mössbauer spectrum of powdered **1** was recorded at 80 K (see Supporting Information, Figure S3). It consists of a doublet with $\delta = 1.31$ mm s^{-1} and $\Delta E_Q = 2.47$ mm s^{-1}. These values are similar to those obtained for other square-pyramidal iron(II) complexes, for example, [Fe$_2$(μ-O$_2$CAr^{Tol})$_3$(4-NCC$_5$H$_4$N)$_2$][BAr′$_4$] ($\delta = 1.04$ mm s^{-1}, $\Delta E_Q = 2.85$ mm s^{-1}; O$_2$CAr^{Tol} = 2,6-di-p-tolylbenzoate, Ar′ = 3,5-bis(trifluoromethyl)phenyl.[11]

Reactivity of 1 in contact with O$_2$: As the malonate binding pockets within **1** are quite basic, the complex is sensitive to moisture, and considering that it contains pentacoordinate Fe^{II} centres with one open coordination site it is not surprising that **1** readily reacts with O$_2$, whereby its colour changes to brown. With respect to the aspects outlined in the introduction, we were interested in how this reaction proceeds and whether it leads to activation of O$_2$ for oxygenation.

After exposing a solid sample of **1** to a dry O$_2$ atmosphere for one week work-up yielded the complex [(Xanthmal)$_2$Fe$_2$O] (**2**), which contains an oxido bridge between two iron(III) centres, as revealed by a single crystal X-ray diffraction study (Figure 2).

In the solid state the molecules exhibit D_{2h} symmetry. The iron ions are located in a distorted square pyramidal coordi-
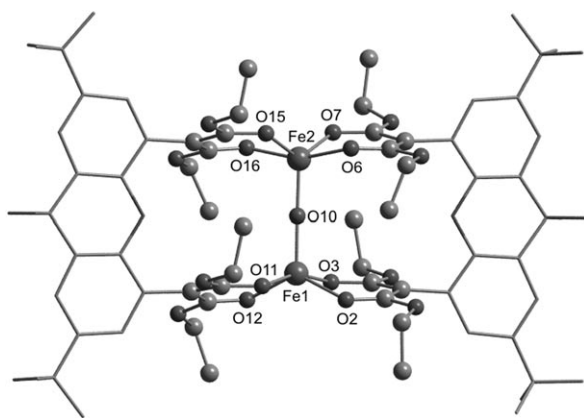
Figure 2. Molecular structure of **2**. All hydrogen atoms and one co-crystallised diethyl ether molecule are omitted for clarity. Selected bond lengths [Å] and angles [°]: Fe1−O10 1.766(2), Fe2−O10 1.760(2), Fe1−O2 1.970(2), Fe1−O3 1.994(2), Fe1−O11 1.986(2), Fe1−O12 1.968(2), Fe2−O6 1.974(2), Fe2−O7 1.972(2), Fe2−O15 1.969(2), Fe2−O16 1.984(2); Fe1-O10-Fe2 177.8(2), O7-Fe2-O6 85.61(7), O2-Fe2-O3 86.17(7).

nation sphere that is composed of the Xanthmal oxygen donor atoms and the bridging oxido ligand. Fe1 is displaced out of the O_4 basal plane by 0.56 Å, and Fe2 by 0.57 Å. The Fe1-O10-Fe2 angle is almost linear (178°), and the Fe−O bond lengths lie within the typical range. All Fe−O$_{Xanthmal}$ bond lengths are very similar and correspond well to the shorter bonds found in **1**. Further comparison of **1** and **2** shows that the C−C and C−O distances in the ligand frameworks vary only in the second decimal place. Temperature-dependent measurement of the magnetic susceptibility of **2** showed antiferromagnetic coupling and the best fit [see Eq. (1)] of the experimental data for two $S = 5/2$ Fe centres gave $J = -110$ cm^{-1} and $g_1 = g_2 = 2.0$.[7,9] The μ_{eff}/T plot and the best fit are shown in Figure S2 (Supporting Information).

Treating solutions of **1** with dioxygen also led to **2**. However, since the yields achieved were reproducibly quite low, chelex was added after one such experiment (performed at −40°C in acetonitrile) to remove all iron, so that subsequently the organic components of the corresponding solution could be investigated. By means of separation by column chromatography and subsequent characterisation with the aid of NMR spectroscopy and mass spectrometry, nine products resulting from ligand oxidation could be identified beside protonated Xanthmal^{2-} (see Scheme 2 and Tables S1 and S2, Supporting Information), which explains the low yields obtained for **2**.

To examine the influence of solvent, temperature and reaction time on the extent of ligand oxidation, the experiment was repeated under various conditions. Relative quantities of the products (vide supra) were determined with the aid of ^{1}H NMR spectroscopy. Table 2 lists for each individual functional group the percentage fraction of all possible functions found in different combinations at the xanthene backbone (i.e. functions are counted independently of the second site) in dependence on the reaction conditions.
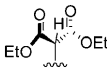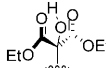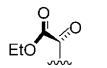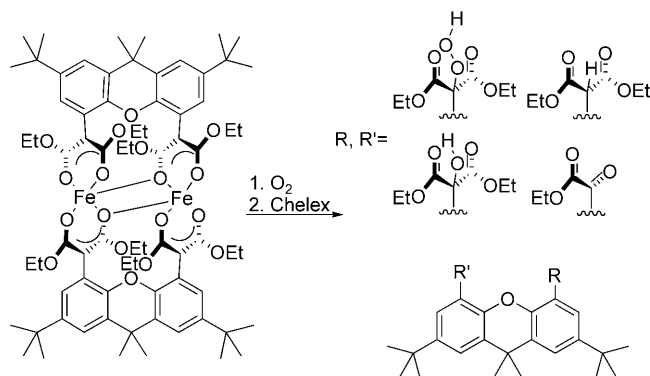

Scheme 2. Reaction of **1** with O_2 and the ten compounds isolated after work-up (all combinations of R and R′).

Table 1. Crystal data and structure refinement for **1** and **2**.

|	**1**·Et$_2$O	**2**·Et$_2$O
formula	C$_{78}$H$_{106}$Fe$_2$O$_{19}$	C$_{78}$H$_{106}$Fe$_2$O$_{20}$
M_r	1459.33	1475.33
$F(000)$	778	1572
T [K]	130(2)	150(2)
crystal system	triclinic	monoclinic
space group	$P\bar{1}$	$P2_1$
a [Å]	11.243(2)	11.2887(6)
b [Å]	12.974(3)	25.6039(11)
c [Å]	14.407(3)	13.7735(7)
α [°]	97.054(14)	90
β [°]	99.107(13)	102.155(4)
γ [°]	109.853(13)	90
V [Å^3]	1916.1(7)	3891.8(3)
Z	1	2
ρ_{calcd} [g cm^{-3}]	1.265	1.259
reflns measured	18059	52058
reflns unique	6707	15161
GOD F^2	1.032	1.032
largest diff. peak/hole [e Å^{-3}]	0.843/−0.491	0.910/−0.633
$R(F)/wR(F^2)$ (all reflns)	0.0997/0.2586	0.0573/0.1405

The third column represents the original malonate binding pocket in the hydrolysed form. No oxidation has occurred in this case, and the corresponding yield therefore can serve as a measure for the conversion achieved. The fourth column shows a group that can only arise in course of an aqueous work-up from a species with an O atom linked to the C_α atom of the binding pocket, probably connected at the same time to the corresponding iron centre. The group shown in the fifth column results from further oxidation of the original binding pocket with C−C bond cleavage, and the last column shows an organohydroperoxide unit. Compounds containing the latter can apparently only be isolated after reactions performed at −40°C, as judged from entries 1–4 of Table 2. Accordingly, at room temperature (and a fortiori at 70°C) they either decompose in the presence of iron or they are not formed in the first place. An excess of O_2 does not seem to aid the formation at −40°C to the extent one would have expected (cf. entries 6 and 7 in Table 2), probably because the solubility of O_2 in

Table 2. Relative "yields of functional groups [%]" generated on exposure of a solution of 29 µmol of **1** in 15 mL of solvent to a dry dioxygen atmosphere. The values are averages for two runs.

Entry	Conditions	E1	E2	E3	E4
1	Et$_2$O, 5 h, RT, 18 equiv O$_2$	79.4	20.6	0.0	0.0
2	MeCN, 5 h, RT, 18 equiv O$_2$	67.7	30.2	2.1	0.0
3	MeCN, 16 h, RT, 18 equiv O$_2$	62.7	33.7	3.6	0.0
4	MeCN, 3 h, 70 °C, 18 equiv O$_2$	44.1	48.5	7.4	0.0
5	MeCN, 16 h, −40 °C, 18 equiv O$_2$	44.2	33.6	9.4	12.8
6	MeCN, 86 h, −40 °C, 18 equiv O$_2$	34.7	37.5	14.6	13.3
7	MeCN, 24 h, −40 °C, 54 equiv O$_2$	36.2	35.5	14.3	13.9
8	MeCN, 86 h, −40 °C, 54 equiv O$_2$	34.1	36.2	14.1	15.7
9	CH$_2$Cl$_2$, 24 h, −40 °C, 54 equiv O$_2$	71.1	24.6	1.3	3.0

ΣR,R′ =

acetonitrile is a limiting factor ($c(O_2) = 4.18 \times 10^{-4}$ mol L^{-1}[12] vs $c(\mathbf{1}) = 19.33 \times 10^{-4}$ mol l^{-1}). Furthermore, Table 2 shows that the selectivity for the mono-oxygenated product (E2) is highest at room temperature. At higher or lower temperatures the relative amounts of α-keto ester and peroxide formed as by-products are higher. Moreover, the reactivity is highest in acetonitrile as solvent, so all further experiments were carried out with this solvent.

Mechanistic considerations: The results described above demonstrate that **1** indeed activates dioxygen so that the reactive species formed oxygenate the ligand.[13] The products obtained point to a complex underlying mechanism that seemed very interesting, both from a general point of view, but also considering the products formed on oxidation of 2,4-pentadiones by the above-mentioned acetylacetone dioxygenase: these are carboxylic acid and pyruvaldehyde derivates, which are proposed to form via an organoperoxo intermediate according to Scheme 3.[14]
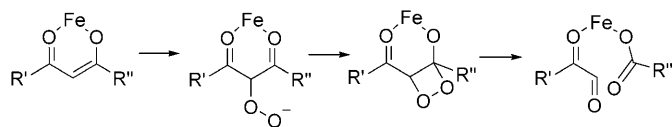
Scheme 3. Proposed mechanism for the cleavage of 2,4-pentadione derivates by enzyme Dke1.

Cleavage of an acetylacetone derivative to yield a substituted pyruvaldehyde is reminiscent of the malonate cleavage leading to the α-keto ester shown in Scheme 2, and hence an investigation of the corresponding mechanism seemed valuable, also in this respect.

The role of Fe^{II} and Fe^{III}: First, the function of iron in the oxidation reaction must be contemplated. As there are literature reports that various alkyl methyl esters, after complex-

ation with alkali metal cations, react in the presence of hexamethylphosphoramide with dioxygen to yield the corresponding 2-hydroperoxy esters,[15] it seemed possible that the iron(II) ions in **1** do not activate the reagent dioxygen through its redox properties but rather the ligand via its Lewis acidic character[16] (O$_2$ would not have to bind to iron then). However, analogous treatment of [(Xanthmal)$_2$Zn$_2$][3] or [(Xanthmal)Li$_2$][3] with O$_2$ did not lead to any conversion, so the first step of the reaction of **1** with dioxygen will consist of its binding to iron. A further important question concerns the role of **2** in the system. Is it an active intermediate or a compound formed in a competitive dead-end route? In fact, active participation is imaginable: Once **2** is formed through initial Fe^{III} superoxido formation and reaction with a further equivalent of **1**, intramolecular ligand-to-metal electron transfers could re-establish the oxidation state +II at the iron centres. Concomitantly, two of the malonate units would be converted to malonyl radicals with the unpaired spin density mainly located at C$_\alpha$ (Scheme 4). In this form the ligand would surely be prone to react with dioxygen as a scavenger, and subsequent steps could lead to compounds whose work-up would give rise to the oxidised compounds found.
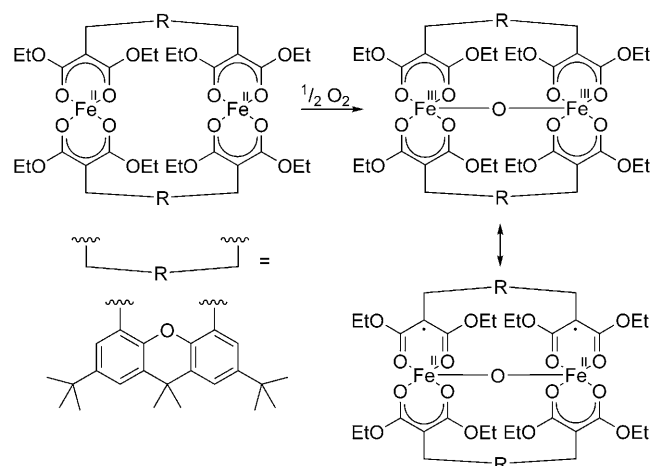
Scheme 4. Conceivable reactivity of **2** that can be excluded.

To clarify whether this is a realistic scenario, several experiments were performed in which **2** was exposed to dioxygen at −40 °C and room temperature in acetonitrile. In none of these cases was any reactivity observed, so oxidation of

the ligand and formation of **2** must represent two concurrent reaction pathways. The oxidation reactions require Fe^{II}.

Mononuclear versus dinuclear reactivity: A further important question for the subsequent mechanistic discussions is whether cooperative binding of O$_2$ by two iron centres is responsible for the observed reactivity, or whether the two iron centres act independently. Therefore, ligand precursor (Xanthmal^{mono})H (**4**) was synthesised and lithiated for subsequent reaction with FeCl$_2$ to yield iron complex [Fe$_2$(Xanthmal^{mono})$_2$] (**6**; Scheme 5), a mononuclear iron
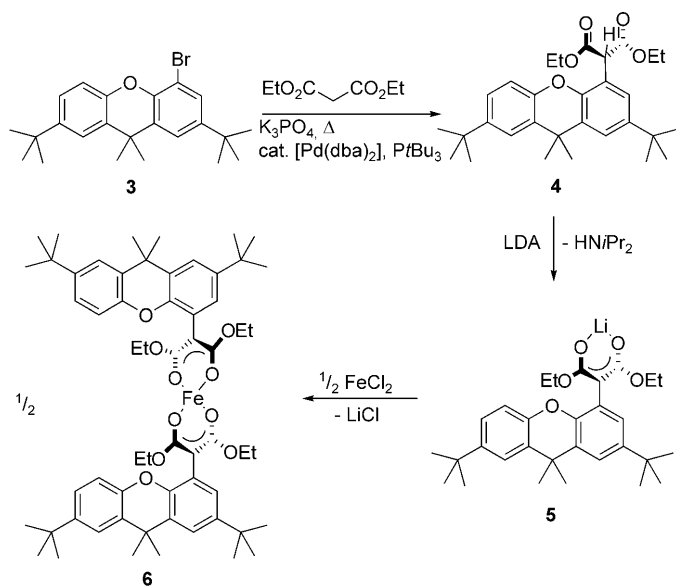

Scheme 5. Synthesis of **6**.

compound comparable to **1**. Even though it was not possible to crystallise **6** and thus confirm its structure by an X-ray diffraction study, this was achieved for a derivative,[17] so we can be sure about the mononuclear character of **1**. Any difference observed in the reactions of **6** with O$_2$ in comparison to **1** should indicate cooperative behaviour of the two iron centres in **1**.

Treating solutions of **6** with O$_2$ leads to only two products of ligand oxidation: alcohol and α-keto ester. A hydroperoxide cannot be isolated after work-up (Scheme 6). The oxidation products were quantified by NMR spectroscopy after removal of all iron ions from the solution. Table 3 lists these quantities in dependence on the reaction conditions.

Comparing entry 3 of Table 3 with entry 7 of Table 2 shows that now the α-keto ester is the main product of the reaction, while alcohols were predominantly isolated after reaction of **1** with O$_2$. This, as well as the fact that even at −40 °C no peroxides are formed, points to a different (mononuclear) mechanism of O$_2$ activation for **6**. This is also supported by the results obtained at room temperature and at 70 °C. At these temperatures the sum of all oxidation products is significantly lower for **6** than for **1**, and the product
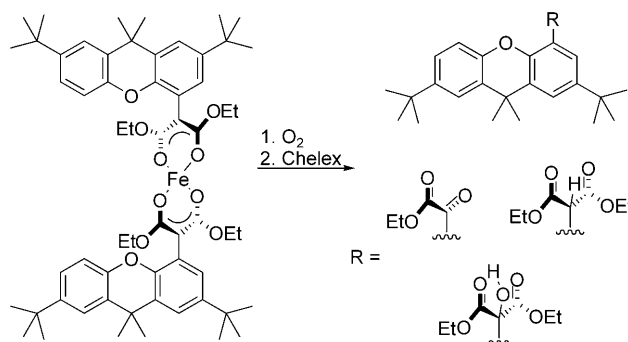

Scheme 6. Reaction of **6** with O$_2$ and the resulting ligand oxidation products.

Table 3. Yields [%] of oxidation products obtained on exposure of a solution of **6** (29 μmol) in acetonitrile (15 mL) to a dry dioxygen atmosphere. The values are averages for two runs.

Entry	Conditions	E1	E2	E3
1	5 h, RT, 9 equiv O$_2$	84.6	6.5	8.9
2	3 h, 70 °C, 9 equiv O$_2$	82.3	11.9	5.8
3	24 h, −40 °C, 27 equiv O$_2$	45.9	22.9	31.2

distribution is different, too. These results suggest that in the case of **1** activation of dioxygen involves cooperative action of both iron centres. A dinuclear route for **6** would require the interaction of two molecules for O$_2$ activation, and thus it should be intrinsically slower than the corresponding reaction of **1**, in which such a situation is prearranged intramolecularly. To test whether there is any contribution at all, the reaction of **6** with O$_2$ was also repeated under diluted conditions (50 mL acetonitrile, 29 μmol of **6**, 24 h at −40 °C, 27 equiv O$_2$). Any dinuclear process should then become even slower, and this should express itself in the product distribution. However, this experiment did not lead to any difference in the distribution of oxidation products, so a dinuclear reaction pathway can be excluded for **6**. The binding of O$_2$ must occur at one Fe centre, presumably through formation of an iron superoxido species. Subsequently, activation is not supported by a second metal centre as in **1**, and this will then most likely lead to attack of the nucleophilic oxygen atom of the Fe^{III} superoxide moiety at the electrophilic C atom of an ester unit with formation of an organoperoxido iron moiety. This kind of reactivity is also found in α-keto acid dependent non-heme iron proteins and model compounds thereof.[18] Such an intermediate could decompose to give an α-keto ester and carbonic acid ester EtOCO$_2^-$ (Scheme 7, route a).[19] On the other hand, the superoxide formed initially can apparently also initiate double monooxygenation of the ligand (Scheme 7, route b),
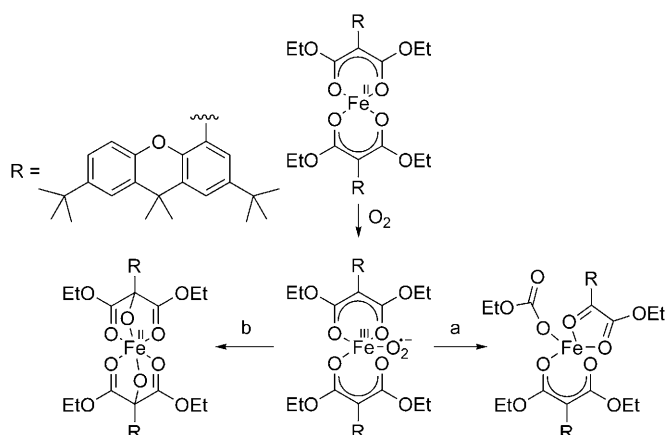
Scheme 7. Oxidation of the ligand via a mononuclear pathway.

but route a seems to be more favourable. Of course, this kind of reactivity can also occur for **1**, but it is only a background process, as the product distribution shows (i.e., the dinuclear route is faster).

Hence, it can be concluded at this stage that both Fe centres of **1** are involved in O₂ activation. Furthermore, it can be inferred that formation of the organoperoxide species (as isolated after the reaction of **1**) also requires two Fe centres and that they do not originate from Fe superoxido species; otherwise, corresponding products should have occurred after reaction of **6**, too. It therefore seemed important to investigate the role of the peroxide intermediates in the formation of the other products.

Peroxide decomposition: When the reaction of [Fe₂-(Xanthmal)₂] (**1**) and dioxygen was monitored by IR spectroscopy at room temperature and −40 °C for 5 h, the bands for ν(C=O/C=C) vibrations at 1646 and 1607 cm⁻¹ as well as the band for ν(C−O) vibration at 1109 cm⁻¹ decreased, while a new ν(C=O) band appeared at 1735 cm⁻¹, which can be explained by monooxygenation of the ligand (Scheme 8).

Assuming that organoperoxido iron units are in fact responsible for E4 of Table 2 in the case of the low-temperature reactions, the question arises whether these also represent the precursors for E2 and E3 or whether the corresponding species are generated via alternative pathways. To study the decomposition of the organoperoxido iron compounds formed initially,[20] a reaction mixture whose work-up in a separate experiment led to the data in entry 7 of Table 2 was degassed. It was then warmed to room temperature and stirred for 24 h in one experiment, while in another
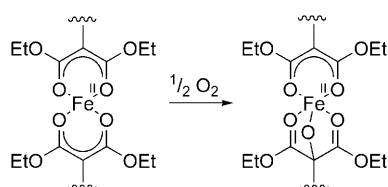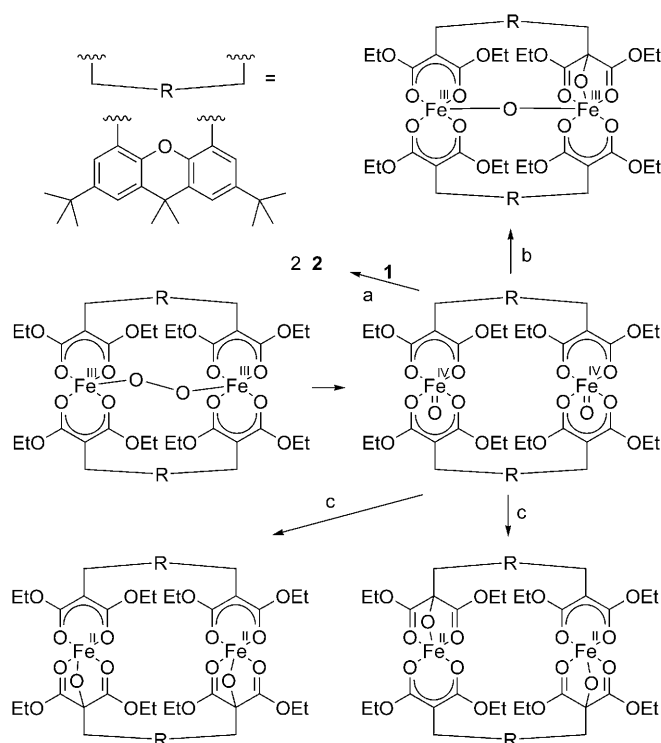
it was stirred at −40 °C for 48 h. Subsequent work-up (see Supporting Information) showed that at room temperature the peroxido species completely decompose to give E2 (78%) and E3 (22%), while decomposition is far slower at −40 °C: only 2% decomposition was observed after 48 h (E2/E3 70/30), which is not sufficient to explain entry 7. Furthermore, it became obvious that peroxide decomposition does not alter the percentage of unconverted malonate, which is noteworthy: As the peroxide contains two O atoms and the corresponding alcohol only one, an oxo atom must be transferred somewhere for each equivalent of alcohol generated in the course of peroxide decomposition, and the receptor is apparently not an unconverted malonate group. It seems unlikely that the rather inert solvent acetonitrile is oxidised.[21] More likely the Feᴵᴵ/Feᴵᴵ unit is oxygenated to a Feᴵᴵᴵ-O-Feᴵᴵᴵ moiety. At that stage reactivity stops, and in consequence only monofunctionalised Xanthmal ligands can be obtained in this way. However, as outlined above the alcohol group occurs also in combination with the other oxidised entities, and accordingly these must form via different pathways. Moreover, at room temperature decomposition of a peroxido intermediate cannot be a major reaction route to E2 either, as the E2/E3 ratio is 94/6, and that does not agree with that found for decomposition of the peroxides at this temperature. Finally, it appears that the overall sum of oxidised ligand functions is decreased by raising the temperature, which is also not in line with a formation route via decomposition of peroxide.

Monooxygenation: Thinking of a more direct route to monooxygenation, it is reasonable to assume initial formation of a Feᴵᴵᴵ superoxido species that is trapped by the neighbouring Feᴵᴵ ion to give a Fe-O-O-Fe moiety (Scheme 9). This kind of reactivity has also been proposed for the sMMO[4] and for several biomimetic model complexes.[22]
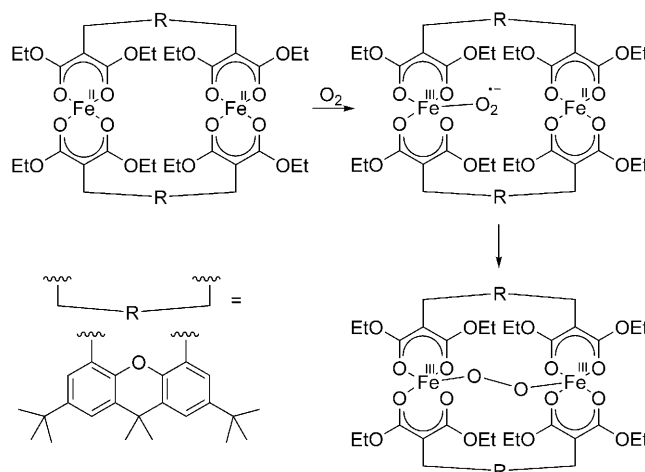
Scheme 9. First steps in the reaction of **1** with dioxygen.

Scheme 8. Mono-oxygenation of Xanthmal²⁻.

The next step could consist of homolytic O−O bond cleavage which would lead to two Feᴵⱽ=O units[23] (Scheme 10),

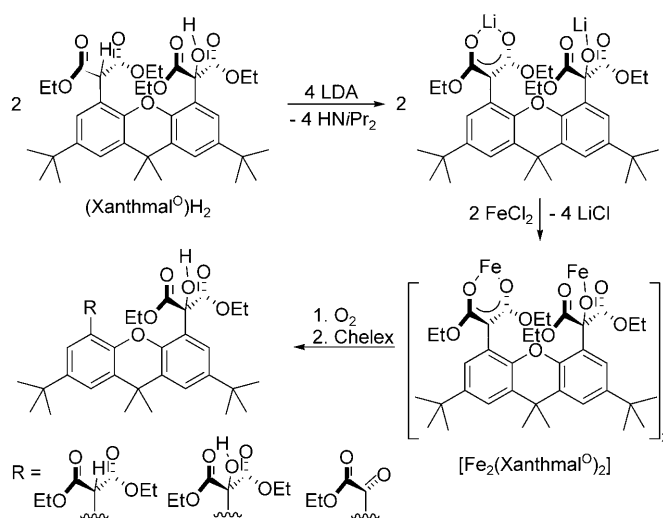Scheme 10. Proceedings after O–O bond cleavage.

Scheme 11. Synthesis of [Fe₂(Xanthmal^O)₂] and its reaction with O₂.

Table 4. Yields of oxygenated ligand generated on exposure of a solution of $[Fe_2(Xanthmal^O)_2]$ (24 μmol) in acetonitrile (10 mL) to a dry dioxygen atmosphere.

Conditions	E1	E2	E3
MeCN, 5 h RT, 18 equiv O_2	83.8	15.0	1.2
MeCN, 24 h −40 °C, 54 equiv O_2	97.8	2.2	0.0

and these should in turn be the active species.[24] Three reaction routes can be envisioned for these: reaction with a further equivalent of **1** should provide two equivalents of **2**, and this is a dead-end route (Scheme 10, route a). Furthermore, it is possible that one Fe^{IV}=O unit mono-oxygenates the ligand while the second establishes an oxido bridge to the neighbouring iron centre (Scheme 10, route b, leading to mono-hydroxylation). This again would lead to a Fe^{III}/Fe^{III} complex that would not show any further reactivity. Finally, it is possible that each Fe^{IV}=O group mono-oxygenates one of the donor functions bound to it in the α-position (route c, leading to 1 equiv of the corresponding diol, or two equivalents of mono-hydroxylated ligand, Scheme 10). Only via route c is a Fe^{II}/Fe^{II} complex reformed that in principal could undergo further O₂ binding reactions analogous to those in Scheme 10 or even more exhaustive oxidation to give compounds that beside an alcohol unit also contain peroxide or ketone groups (as listed individually in Tables S1 and S2, Supporting Information).

Peroxide and ketone formation: To test whether a monooxygenated ligand can indeed be oxidised further, the isolated monohydroxylated compound (Xanthmal^O)H₂ (see Supporting Information) was allowed to react with LDA, and the resulting lithium salt with FeCl₂ (Scheme 11). The iron complex formed was then treated with O₂ at room temperature and −40 °C. The oxidation products identified after work-up are shown in Table 4.

The results suggest that the oxygenated species formed via route c in Scheme 10 is not a precursor for peroxides or

doubly oxygenated products at −40 °C.[26] Apparently, monooxygenation leads to deactivation, and only at room temperature is further oxidation observed. Hence, a fundamentally different mechanism for ketone and peroxide is required to explain the presence of these functional groups beside alcohol units in the products.

Going back to the Fe^{IV}=O/Fe^{IV}=O species formed after homoleptic O–O bond cleavage, as shown in Scheme 10, a further (additional) reaction route seems plausible: Certainly, such a high-valent species would stabilise itself through electron transfer from the ligand π system to the highly oxidised Fe^{IV} centres,[27] which would lead to Fe^{III} ions and a ligand-centred radical (Scheme 12).

The radical would be prone to attack by the diradical O₂, which would lead to an organoperoxide radical. Such trapping has also been suggested to initiate the activity of acetylacetone dioxygenase,[14a] and by analogy to the processes proposed for it in Scheme 3 subsequent reactions can be envisioned for the organoperoxo intermediate derived from **1** that lead to the corresponding α-keto esters (route e in Scheme 13). Alternatively, the organoperoxide species could react to give an organoperoxido iron(IV) species
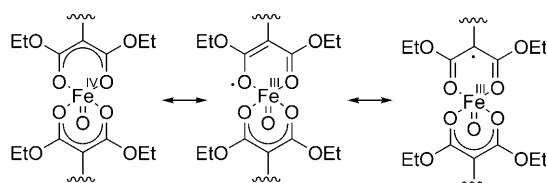
Scheme 12. Intramolecular electron transfer from the ligand to the Fe^{IV} centre.

(Scheme 13, route f), which would be the source of E4 in Table 2. Decomposition of the organoperoxido iron units can be imagined to yield complexes that also contribute to E2 and E3 in Table 2, albeit only to a small extent according to the results described under "peroxide decomposition". In any case, ketone formation should be accompanied by formation of one equivalent of complexed EtOCO$_2^-$, which could be anticipated to eliminate CO$_2$. However, liberation of CO$_2$ was not observed during the reaction, while EtOH could be detected among the products after work-up, so we assume decomposition of EtOCO$_2^-$ at this stage. Scheme 13 summarises all mechanistic suggestions gathered on basis of the experimental data for the system **1**/O$_2$ at −40 °C: Reaction route c (monooxygenation of the ligand) as well as routes a and b (to the Fe^{III} compounds) of the Fe^{IV}=O unit compete with reactivity based on the Fe^{III}/radical unit (d followed by e or f). The latter can occur at one of the malonate units independently of the other, which accounts for all permutations of functional groups shown in Table 2 at one xanthene backbone.

To get information on product formation in dependence on time, reactions at −40 °C were interrupted after different periods of time and the products formed until then determined. This revealed that a conversion of about 55 % is reached over the first 17 h, while conversion of the next 10 % takes about 85 h, that is, the oxidation of the ligand cannot be driven to completion within a reasonable time window, presumably due to deactivation through route c in Scheme 13 and formation of Fe^{III} species (routes a and b). A closer look at the individual compounds formed (see Supporting Information), reveals that the proportion of monofunctionalised compounds increases during the first 2–3 h and then decreases again in favour of bifunctionalised ones, and this is reasonable if a sufficiently long lifetime of the O=Fe^{III}/radical intermediates is assumed. On this basis one would envision that addition of a radical trap should prohib-
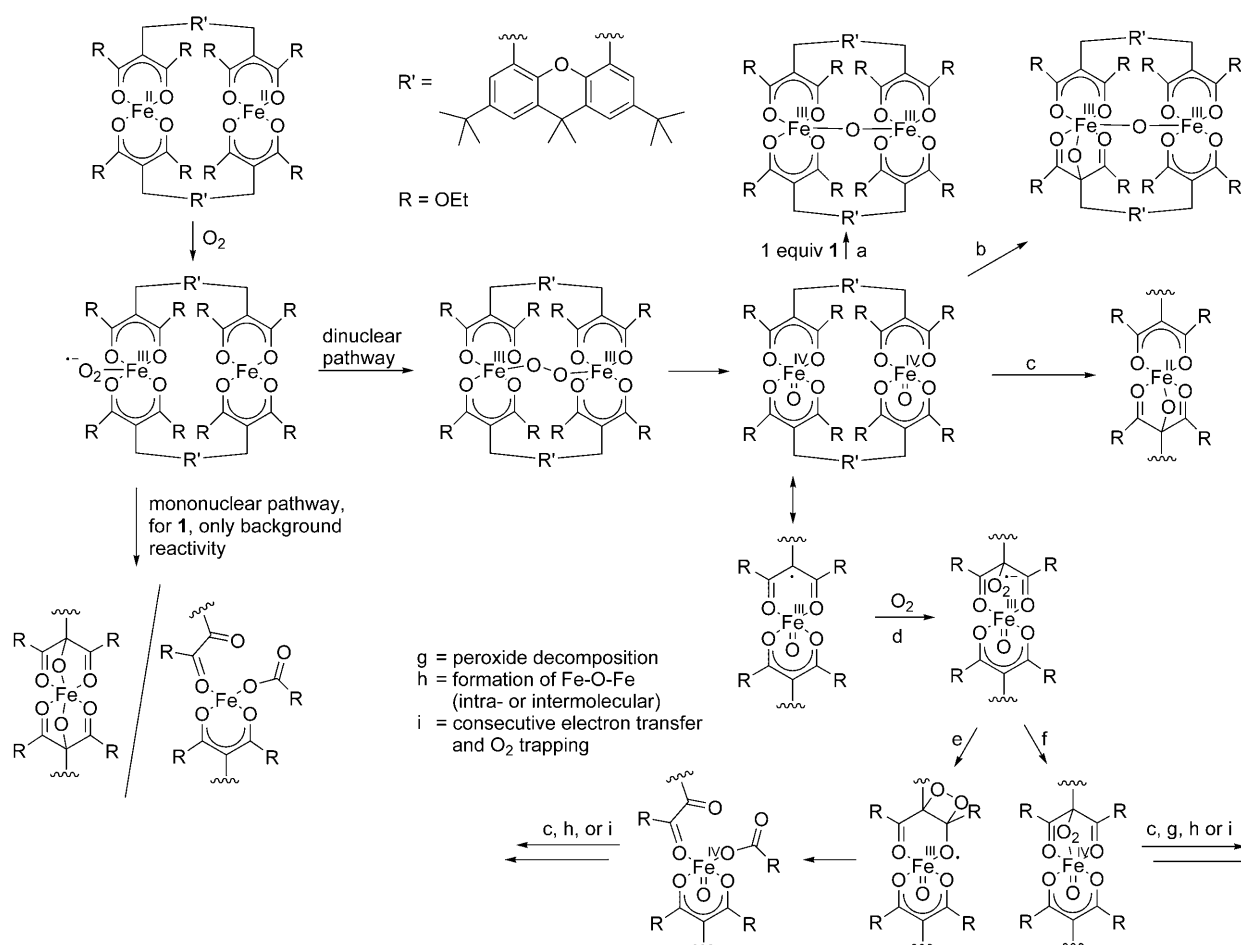
Scheme 13. Summary of the mechanism for the reactivity of **1** in contact with O$_2$ at −40 °C and subsequent processes. Reactions shown for only one site can also occur in parallel at the other (grey).
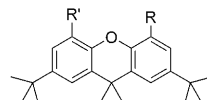
it peroxide and thus also ketone formation; secondly, the yield of alcohols should significantly decrease. However, it proved difficult to find a radical trap that 1) is not protic (protons hydrolyse **1**), 2) does not react with O_2 or $O_2^{\cdot -}$ und thus prohibits reactivity, 3) does not initiate radical reactions itself and 4) does not coordinate strongly. For instance, we employed NO which, however, undergoes redox reactions with **1**, and $CBrCl_3$ similarly reacts with **1** before O_2 addition, perhaps because it is a radical starter, too. The most convincing results were obtained after addition of naphthyl-phenylamine,[28] whose presence (290 µmol in 20 mL aceto-nitrile containing 29 µmol of **1**) during the reaction with O_2 led to selective formation of the mono-oxygenated ligand and decreased reactivity (work-up after 24 h at −40 °C in the presence of 54 equiv O_2 gave 17.5 % (Xanthmal^O)H$_2$). Although it is usually difficult to compete with intramolecular ligand oxidation if this occurs readily, we also tried to perform reactions of the high-valent intermediates with external substrates to gain further evidence of their existence. Hence, the reaction of **1** with O_2 was performed in the presence of a thousandfold excess of cyclooctene at room temperature and −40 °C. At room temperature one oxo atom per four equivalents of **1** was transferred to cyclooctene to give cyclooctene epoxide, and at −40 °C only traces of cyclooctene epoxide were detected. In both reactions, no diol was observed among the products.
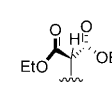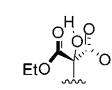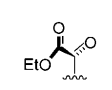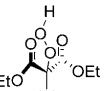
Reaction at room temperature: Having derived a plausible mechanism for the reactivity of **1** with dioxygen at −40 °C the question remains why the yields of oxygenated products decrease at room temperature while the selectivity with respect to alcohol functional groups increases. A possible explanation would be that at room temperature the $Fe^{IV}=O$ or $Fe^{III}=O$/radical intermediates react more rapidly along the lines of routes a–c in Scheme 13, and therefore the bimolecular reaction with O_2 (present only in low concentrations, vide supra) according to route d in Scheme 13 has less room for development, that is, less ketone is formed. The lower overall yields observed can be understood by taking into account that routes a and b utilise the activated oxygen for the formation of Fe-O-Fe units, and this oxygen as well as the corresponding Fe sites are lost for ligand oxidation. To test this hypothesis the reaction of **1** at room temperature was followed in dependence on time. In line with the above arguments, the main part of the oxidation products observed after 16 h had already formed after 30 min, that is, reactions in Scheme 10 are accelerated and the smaller extent of conversion is due to more rapid formation of Fe-O-Fe units.

Catalysis: Following route c in Scheme 13, it can be noted that after ligand oxidation the iron centre is back in the oxidation state +II, and the same is true for routes e and f if they are followed by route c. Thus, in principle a catalytic conversion should be possible. To test this hypothesis a mixture of **1** and [(Xanthmal)Li$_2$] in the ratio of 1:20 was treated in the usual way with O_2, and the yields of oxidation products were determined. The results are summarised in Table 5, and they show that indeed catalytic conversion occurs.

Table 5. Relative "yields of functional groups [%]" generated on exposure of a solution of **1** (2.7 µmol) and [(Xanthmal)Li$_2$] (54 µmol) in acetonitrile (15 mL) to a dry dioxygen atmosphere (36 equiv) for 5 h. The values are averages for two runs.

Conditions	ΣR,R′ =			
	E1	E2	E3	E4
RT	26.1	67.3	0.0	6.6
−40 °C	60.3	38.6	0.0	1.1

Apparently, directly after functionalisation of a ligand it is replaced by an unchanged ligand. This reactivates the iron centres after one process of oxidation for another one. As immediate replacement also occurs for peroxide formed via route f, peroxide isolation now also becomes possible after reaction at room temperature.[20] The small amounts of peroxides formed confirm again that monooxygenation is the fastest reaction type, but the complete absence of ketones among the products is unexpected on the basis of the previous results, and the preferred formation of peroxides at room temperature remains unclear, too. A possible explanation would be that the catalytic conditions introduce a novel aspect, for example, formation of an "ate complex", or binding of a "substrate ligand" only by one functional group. The fact that catalysis can also be achieved at room temperature (only 26 % of all original malonate groups remained untouched, i.e., TON = 17 per Fe centre) shows that under these conditions the routes of Scheme 13 that lead to Fe^{III} are slow in comparison to single or double monooxygenation of the ligand (Fe^{III} would mean the end of catalysis); for instance, a possible explanation for the suppression of route a (requiring a second equivalent of **1**) would be the significantly decreased concentration of **1** under catalytic conditions. It is then consistent (also considering the previous results for the stoichiometric reactions) that the TON for oxygenation at room temperature is higher than at −40 °C. The occurrence of peroxides in entry 1 of Table 5 provides evidence that, as we assumed above, these in fact also form at room temperature but quickly decompose if they remain bound to iron. Here, in the catalytic experiment, they could be identified, since directly after their formation pristine ligand replaces them at the Fe centres, so that their decomposition is prohibited.[20]

Conclusion

Employing the ligand Xanthmal^{2-} we synthesized a dinuclear Fe^{II} complex that can activate O$_2$ by cooperative action of both Fe centres. This leads to subsequent reactions in the course of which the ligand donor groups are oxygenated: the original malonate units are oxygenated or peroxygenated at the C$_\alpha$ positions and a further pathway leads to α-keto ester groups. The results of a detailed mechanistic investigation suggest that these reactions proceed via intermediate formation of oxidoiron(IV) units which can directly hydroxylate ligand functions. Alternatively, they initiate ligand-to-metal electron transfer followed by trapping of O$_2$. Formation of Fe-O-Fe units, which leads to a deactivation of the system, is effectively suppressed at −40°C but becomes more prominent at room temperature. Investigations on a comparable mononuclear system confirmed that indeed both Fe centres are required to give the observed reactivity. Consistent with the mechanistic proposal deduced both for room temperature and −40°C, ligand oxidation can also be performed in a catalytic fashion. While this is not a reaction that leads to valuable products, the study of the entire system revealed interesting basic mechanistic steps that in four instances are also biomimetic (Fe-O-O-Fe formation: sMMOH; ligand-to-metal electron transfer and subsequent O$_2$ trapping: catechol dioxygenases; FeO$_2$ attack at complexed carbonyl groups: α-keto acid dependent non-heme iron enzymes; product formation: acetylacetone dioxygenase). The findings thus contribute to a more comprehensive understanding of biological and biomimetic systems and help to establish the rational design of bio-inspired catalysts.

Experimental Section

General considerations and physical methods: All manipulations except for the synthesis of **4** were carried out in a glove box or by means of Schlenk-type techniques under a dry argon atmosphere. The ^{1}H and ^{13}C NMR spectra were recorded on a Bruker AV 400 NMR spectrometer (^{1}H 400.13 MHz; ^{13}C 100.63 MHz) with CDCl$_3$ or CD$_3$CN as solvent at 20°C. The ^{1}H and ^{13}C NMR spectra were calibrated against the residual proton and natural-abundance ^{13}C resonances of the deuterated solvent (CDCl$_3$ $\delta_H = 7.26$ ppm and CD$_3$CN $\delta_H = 1.94$ ppm). Microanalyses were performed on a Leco CHNS-932 elemental analyser. Infrared (IR) spectra were recorded on samples prepared as KBr pellets with a Digilab Excalibur FTS 4000 FTIR spectrometer. Mass spectra were recorded on a Varian MAT311A/AMD (ESI). Temperature-dependent magnetic data were measured with a Quantum-Design MPMS-5S SQUID magnetometer equipped with a 5 T magnet. The powdered samples were contained in a gel bucket and fixed in a nonmagnetic sample holder. Each raw data file for the measured magnetic moment was corrected for the diamagnetic contribution from the sample holder, the gel bucket and the sample. Mössbauer spectra were recorded with a ^{57}Co source in a Rh matrix on a Wissel Mössbauer spectrometer equipped with a Janis closed-cycle helium cryostat. Isomer shifts are given relative to iron metal at ambient temperature. Simulation of the experimental data was performed with the Mfit program (E. Bill, Max-Planck Institute for Bioinorganic Chemistry, Mülheim/Ruhr, Germany).

X-ray structure determination: The crystals were mounted on a glass fibre and then transferred into the cold nitrogen gas stream of a Stoe IPDS2T diffractometer equipped with Mo$_{K\alpha}$ radiation ($\lambda = 0.71073$ Å).

The structures were solved by direct methods (SIR 2004)[29] and refined versus F^2 (SHELXL-97)[30] with anisotropic temperature factors for all non-hydrogen atoms (Table 1). All hydrogen atoms were added geometrically and refined by using a riding model. CCDC-684680 (**2**), CCDC-684681 (**1**·2MeCN) and CCDC-684682 (**1**) contain the supplementary crystallographic data for this paper. These data can be obtained free of charge from The Cambridge Crystallographic Data Centre via www.ccdc.cam.ac.uk/data_request/cif.

Materials: Solvents were purified, dried and degassed prior to use. Chelex, an iminodiacetic acid based ion exchanger, was purchased from Sigma. [Fe(OTf)$_2$(MeCN)$_2$],[31] Fe[N(SiMe$_3$)$_2$]$_2$(thf)$_2$,[32] 4-Bromo-2,7-di-*tert*-butyl-9,9-dimethylxanthene (**3**),[33] LDA and [(Xanthmal)Li$_2$][3] were prepared according to the literature procedure.

Synthesis

Bis(κ^2-*O*,*O*-(4,5-bis(1′3′-ethoxy-1′,3′-propanedionyl)-2,7-di-*tert*-butyl-9,9-dimethylxanthenato-diiron(II), [Fe$_2$(Xanthmal)$_2$] (1)

Method 1: One equivalent of FeCl$_2$ or [Fe(OTf)$_2$(MeCN)$_2$] was added to a suspension of one equivalent of [(Xanthmal)Li$_2$] in THF and the mixture stirred for 14 h at room temperature. Subsequently, the white precipitate was separated by filtration and washed twice with THF (15 mL). After drying in vacuo, **1** was obtained as a white powder in yields of 63 and 70%, respectively.

Method 2: Fe[N(SiMe$_3$)$_2$]$_2$(thf)$_2$ (823 mg, 1.58 mmol) was added to a solution of (Xanthmal)H$_2$ (1.00 g, 1.58 mmol) in THF and the mixture stirred for 14 h. After removal of all volatile materials in vacuo the product was isolated as described above; yield: 394 mg (0.284 mmol, 36.0%). Crystals of **1** suitable for single-crystal X-ray diffraction were obtained by slow evaporation of solvent from a saturated diethyl ether solution. IR: $\tilde{\nu} =$ 2964 (s), 2903 (m), 2869 (w), 1636 (vs), 1612 (vs), 1479 (vs), 1464 (vs), 1444 (vs), 1406 (vs), 1376 (vs), 1333 (vs), 1294 (m), 1275 (m), 1242 (m), 1205 (vw), 1168 (w), 1102 (vs), 1073 (m), 1047 (vw), 894 (vw), 874 (w), 857 (vw), 789 (w), 742 (vw) cm^{-1}; elemental analysis calcd (%) for C$_{74}$H$_{96}$O$_{10}$Fe$_2$: (1385.23): C 64.16, H 6.99; found: C 63.91, H 7.30.

Bis(κ^2-*O*,*O*-(4,5-bis(1′3′-ethoxy-1′,3′-propanedionyl)-2,7-di-*tert*-butyl-9,9-dimethylxanthenato-μ-oxidodiiron(II) (2)

Method 1: Dioxygen (12 mL) was added to a solution of **1** (338 mg, 0.244 mmol) in dichloromethane at −30°C. Over 5 h the reaction mixture was warmed to ambient temperature and stirred for a further 2 h. The solvent was removed in vacuo and diethyl ether (20 mL) was added. The resulting suspension was filtered, and the brown residue was dissolved in diethyl ether. Analytically pure crystals of [(Xanthmal)$_2$Fe$_2$O]·Et$_2$O were obtained by slow evaporation of the solvent from this solution. Yield: 50 mg (14%).

Method 2: Dioxygen (40 mL) was added to 100 mg of powered **1** (72.1 μmol). After one week dioxygen was removed and the brown powder was dissolved in diethyl ether (15 mL). Analytically pure crystals of [(Xanthmal)$_2$Fe$_2$O]·Et$_2$O were obtained by slow evaporation of the solvent from this saturated solution. Yield: 30% (32 mg, 21.3 μmol). IR: $\tilde{\nu} =$ 2963 (s), 2932 (m), 2868 (w), 1604 (vs), 1456 (s), 1439 (s), 1410 (m), 1381 (s), 1308 (w), 1288 (w), 1238 (w), 1169 (w), 1111 (vs), 897 (vw), 858 (vw), 795 (vw) cm^{-1}; elemental analysis calcd (%) for C$_{78}$H$_{106}$O$_{20}$Fe$_2$ (1475.35): 63.50, H 7.54; found C 63.30, H 7.54.

4-(1′,3′-Ethoxy-1′,3′-propanedionyl)-2,7-di-*tert*-butyl-9,9-dimethylxanthene (4): Diethyl malonate (3.8 mL, 23 mmol) was added to a suspension of **3** (8.45 g, 21.1 mmol), K$_3$PO$_4$ (11.2 g, 53 mmol), [Pd(*trans,trans*-dibenzylideneacetone)$_2$] (303 mg 0.527 mmol) and P*t*Bu$_3$ (214 mg, 1.06 mmol) in toluene (50 mL) at RT under an argon atmosphere with exclusion of light. The resulting suspension was heated for 15 h at 70°C. Subsequently, the insoluble residue was removed by filtration over Celite. After removal of all volatile substances from the filtrate in vacuo the residual yellow oil was purified by column chromatography on silica gel with petroleum ether (40/60)/EtOAc (10/1) as eluent. After removal of all volatile substances **4** (7.88 g, 15.9 mmol, 75.4%) was obtained as a white powder. ^{1}H NMR (CDCl$_3$): $\delta = 1.28$ (t, J(H,H) $= 7.2$ Hz, 6H; OCH$_2$C*H$_3$*), 1.32 (s, 9H; C(CH$_3$)$_3$), 1.33 (s, 9H; C(CH$_3$)$_3$), 1.63 (s, 6H; C-(CH$_3$)$_2$), 4.25 (q, J(H,H) $= 7.1$ Hz, 2H; OC*H$_2$*-CH$_3$), 5.25 (s, 1H; CH-(CO$_2$Et)$_2$), 7.20 (dd, J(H,H) $= 8.5$, 2.4 Hz, 1H; CH$_{Ar}$), 7.20 (d, J(H,H) =

2.3 Hz, 1H; CH$_{Ar}$), 7.25 (d, J(H,H)=2.3 Hz, 1H; CH$_{Ar}$), 7.29 ppm (m, 2H; CH$_{Ar}$); ^{13}C{^{1}H} NMR (CDCl$_3$): δ=14.1 (OCH$_2$CH$_3$), 31.5 (C(CH$_3$)$_3$), 31.5 (C(CH$_3$)$_3$), 32.1 (C(CH$_3$)$_2$), 34.5 (C$_{quat}$), 34.5 (C$_{quat}$), 34.6 (C$_{quat}$), 51.8 (CH(CO$_2$Et)$_2$), 61.6 (OCH$_2$CH$_3$), 115.6 (CH$_{Ar}$), 119.7 (C$_{quat}$), 122.4 (CH$_{Ar}$), 122.5 (CH$_{Ar}$), 124.2 (CH$_{Ar}$), 124.6 (C$_{Ar}$), 129.3 (CH$_{Ar}$), 129.4 (C$_{Ar}$), 144.8 (C$_{Ar}$), 145.8 (C$_{Ar}$), 146.1 (C$_{Ar}$), 148.1 (C$_{Ar}$), 168.6 ppm (COOEt$_2$); HRMS (ESI): m/z: 481.2949 [M+H]$^+$ (calcd: 481.2949), 503.2768 [M+Na]$^+$ (calcd: 503.2768); IR: $\tilde{\nu}$=2961 (s), 2903 (m), 2867 (w), 1749 (vs), 1728 (vs), 1502 (m), 1466 (vs), 1406 (m), 1362 (s), 1313 (vs), 1292 (s), 1225 (s), 1205 (s), 1194 (m), 1171 (m), 1184 (s), 1111 (m), 1086 (w), 1038 (m), 1030 (m), 829 (m) cm^{-1}; elemental analysis calcd (%) for C$_{30}$H$_{40}$O$_5$ (480.64): C: 74.97, H 8.39; found C 74.74, H 8.25.

Bis(κ^2-O,O-(4-(1′3′-ethoxy-1′,3′-propanedionyl)-2,7-di-*tert*-butyl-9,9-dimethylxanthenatolithium (5): LDA (657 mg, 6.13 mmol) was added to a solution of **4** (2.95 g, 6.14 mmol) in THF (50 mL) and the mixture stirred for 14 h at room temperature. After removal of all volatile components in vacuo the residual yellow solid was washed twice with diethyl ether/ hexane (2/1, 60 mL). The remaining white powder was dried in vacuo to obtain **5** (2.09 g, 4.29 mmol, 70%). ^{1}H NMR (CD$_3$CN): δ=0.96 (t, J-(H,H)=7.1, 6H; OCH$_2$CH$_3$), 1.31 (s, 18H; C(CH$_3$)$_3$), 1.61 (s, 6H; C-(CH$_3$)$_2$), 4.92 (m, 4H; OCH$_2$CH$_3$), 6.79 (d, J(H,H)=8.5 Hz, 1H; CH$_{Ar}$), 7.09 (d, J(H,H)=2.5 Hz, 1H; CH$_{Ar}$), 7.23 (d, J(H,H)=2.5 Hz, 1H; CH$_{Ar}$), 7.48 ppm (d, J(H,H)=2.4 Hz, 2H; CH$_{Ar}$); IR: $\tilde{\nu}$=2964 (s), 2905 (m), 2870 (w), 1616 (vs), 1505 (s), 1458 (vs), 1419 (m), 1406 (s), 1377 (s), 1364 (m),1331 (vs), 1292 (m), 1271 (m), 1244 (m), 1231 (w), 1165 (w), 1095 (vs), 1040 (w), 858 (vw), 798 (w) cm^{-1}.

Bis(κ^2-O,O-(4-(1′3′-ethoxy-1′,3′-propanedionyl)-2,7-di-*tert*-butyl-9,9-dimethylxanthenatoiron(II) (6): FeCl$_2$ (260 mg, 2.05 mmol) were added to a suspension of **5** (2.000 g, 4.11 mmol) in THF (30 mL) and the mixture stirred for 14 h at room temperature. Subsequently, all volatile components were removed in vacuo and **6** was extracted with hexane (60 mL). After removing the solvent and drying in vacuo **6** was obtained as an off-white powder in 50% yield (1.04 g, 1.03 mmol). IR: $\tilde{\nu}$=2964 (s), 2907 (m), 2868 (m), 1607 (s), 1501 (m), 1458 (s), 1408 (m), 1377 (m), 1361 (w), 1335 (s), 1292 (m), 1264 (m), 1244 (m), 1169 (w), 1026 (m), 860 (vw), 1103 (vs) 800 (m) cm^{-1}; elemental analysis calcd (%) for C$_{60}$H$_{78}$FeO$_{10}$ (1014.49): C 70.99, H 7.74; found C 71.03, H 7.69.

Protocol for oxidation studies on 1 and 6 with dioxygen in solution: **1** or **6** (29 μmol) was suspended in 15 mL of solvent as specified in Table 2. After cooling/heating of the suspension to the indicated temperature, 18 equivalents of dioxygen in the case of **1** and 9 equivalents of dioxygen in the case of **6** were added by via syringe. In the cases of entry 7 in Table 2 after 11 and 23 h, and entries 5 and 8 in Table 2 after 5 and 10 h, an additional 18/9 equivalents of dioxygen were added to the solution. The solvent was removed in vacuo after the denoted time and diethyl ether (20 mL) and chelex (1 g) was added. After stirring for 2 h the solution was filtered and the residue washed with diethyl ether (10 mL). The solution was evaporated to dryness in vacuo and the resulting residue was dissolved in CDCl$_3$ (0.6 mL). To determine the ratio of the products, ^{1}H NMR spectra of the CDCl$_3$ solutions were recorded (see Supporting Information).

Protocol for catalytic oxidation studies with 1: Compound **1** (3.8 mg, 2.7 μmol) and [(Xanthmal)Li$_2$] (35 mg, 54 μmol) were suspended in acetonitrile (15 mL). After cooling/heating the suspension to the indicated temperature, 9 equivalents of dioxygen were added by syringe. After 5 h the solvent was removed in vacuo and diethyl ether (20 mL) and dilute HCl (0.1 mL) and chelex (1 g) were added. After stirring for 2 h the solution was filtered and the residue washed with diethyl ether (10 mL). The solution was evaporated to dryness in vacuo and the whole residue was dissolved in CDCl$_3$ (0.6 mL). To determine the ratio of the products, ^{1}H NMR spectra of the CDCl$_3$ solutions were recorded (see Supporting Information).

The spectroscopic data of the 11 oxidation products of **1** and **6**, the distributions of the oxidation products according to their functional groups from the catalytic, stoichiometric and time-dependent reactions, as well as the ratios of products from the decompositions of the organoperoxido iron species are provided in the Supporting Information, and the experi-mental data and the best fit of the magnetic measurements of **1** and **2** and the Mössbauer data of **1** are shown graphically.

[1] A. Gavrilova, B. Bosnich, *Chem. Rev.* **2004**, *104*, 349–384; compare for Fe: J. M. Smith, R. L. Lachicotte, K. A. Pittard, T. R. Cundari, G. Lukat-Rodgers, K. R. Rodgers, P. L. Holland, *J. Am. Chem. Soc.* **2001**, *123*, 9222–9223; Zn: G. W. Coates, D. R. Moore, *Angew. Chem.* **2004**, *116*, 6784–6806; *Angew. Chem. Int. Ed.* **2004**, *43*, 6618–6639; B. Bauer-Siebenlist, S. Dechert, F. Meyer, *Chem. Eur. J.* **2005**, *11*, 5343–5352; Cu: A. M. Reynolds, E. A. Lewis, N. W. Aboelella, W. B. Tolman, *Chem. Commun.* **2005**, 2014–2016; V: E. Hoppe, C. Limberg, *Chem. Eur. J.* **2007**, *13*, 7006–7016.

[2] *Comprehensive Coordination Chemistry II, Vol. 8* (Eds.: J. A. McCleverty, T. J. Meyer), Elsevier, Oxford, **2004**, Chaps. 8.1, 8.10, 8.13, 8.15, 8.19, 8.24.

[3] I. Siewert, C. Limberg, *Z. Naturforsch. B* **2007**, *62*, 1251–1258.

[4] M. Merkx, D. A. Kopp, M. H. Sazinsky, J. L. Blazyk, J. Müller, S. J. Lippard, *Angew. Chem.* **2001**, *113*, 2860–2888; *Angew. Chem. Int. Ed.* **2001**, *40*, 2782–2807.

[5] G. Straganz, L. Brecker, H.-J. Weber, W. Steiner, D. W. Ribbons *Biochem. Biophys Res. Comm.* **2002**, *297*, 232–236; G. D. Straganz, A. Glieder, L. Brecker, D. W. Ribbons, W. Steiner, *Biochem. J.* **2003**, *369*, 573–581.

[6] M. F. Pilz, C. Limberg, S. Demeshko, F. Meyer, B. Ziemer, *Dalton Trans.* **2008**, 1917–1923.

[7] Temperature-dependent measurements of the magnetic susceptibility of **1** and **2** were carried out on powdered samples in the temperature range 295–2 K in fields of 2000 and 5000 G. No significant field dependence was observed.

[8] O. Kahn, *Molecular Magnetism*, Wiley-VCH, ## **1993**.

[9] Simulation of the experimental magnetic data with a full-matrix diagonalisation of exchange coupling, Zeeman splitting and zero-field splitting was performed with the julX program: E. Bill, Max-Planck Institute for Bioinorganic Chemistry, Mülheim/Ruhr, Germany. A paramagnetic impurity with Curie–Weiss behaviour (ρ) and temperature-independent paramagnetism (TIP) were included according to $\chi=(1-\rho)\chi+\rho\chi_{mono}$+TIP. For **1**: TIP$=2.5\times10^{-3}$ cm^{3}mol^{-1}, ρ=0.3%; for **2**: TIP$=5.5\times10^{-4}$ cm^{3}mol^{-1}, ρ=0.6%.

[10] S. Pluver, W. A. Froland, B. G. Fox, J. D. Lipscomb, E. I. Solomon, *J. Am. Chem. Soc.* **1993**, *115*, 12409–12422.

[11] S. Yoon, S. J. Lippard, *J. Am. Chem. Soc.* **2005**, *127*, 8386–8397.

[12] Y. Che, K. Tokuda, T. Ohsaka, *Bull. Chem. Soc. Jpn.* **1998**, *71*, 651–656.

[13] Examples of ligand oxidation mediated by iron centres: S. Ménage, J.-B. Galey, G. Hussler, M. Seité, M. Fontecave, *Angew. Chem.* **1996**, *108*, 2535–2537; *Angew. Chem. Int. Ed. Engl.* **1996**, *35*, 2353–2355; E. L. Hegg, R. Y. N. Ho, L. Que, Jr., *J. Am. Chem. Soc.* **1999**, *121*, 1972–1973; D. Lee, S. J. Lippard, *Inorg. Chem.* **2002**, *41*, 827–837; M. Ostermeier, C. Limberg, B. Ziemer, V. Karunakaran, *Angew. Chem.* **2007**, *119*, 5423–5426; *Angew. Chem. Int. Ed.* **2007**, *46*, 5329–5331; M. Yamashita, H. Furutachi, T. Tosha, S. Fujinami, W. Saito, Y. Maeda, K. Takahasi, K. Tanaka, T. Kitagawa, M. Suzuki, *J. Am. Chem. Soc.* **2007**, *129*, 2–3.

[14] a) G. D. Straganz, H. Hofer, W. Steiner, B. Nidetzky, *J. Am. Chem. Soc.* **2004**, *126*, 12202–12203; b) D. Straganz, B. Nidetzky, *J. Am. Chem. Soc.* **2005**, *127*, 12306–12314.

[15] D. A. Konen, L. S. Silbert, P. E. Pfeiffer, *J. Org. Chem.* **1975**, *40*, 3253–3258.

[16] C. Schwarz, D. Schröder, H Schwarz, *Chem. Eur. J.* **2005**, *11*, 619–627.

[17] Results will be reported elsewhere.

[18] L. Que, Jr., R. Y. N. Ho, *Chem. Rev.* **1996**, *96*, 2607–2624; M. Costas, M. P. Mehn, M. P. Jensen, L. Que, Jr., *Chem. Rev.* **2004**, *104*, 939–986; M. Abu-Omar, A. Loaizo, N. Hontzeas, *Chem. Rev.* **2005**, *105*, 2227–2252.

[19] It has been confirmed that the hydroxylated ligand does not undergo any further reaction with O_2 in the presence of iron to yield the α-keto ester.

[20] The corresponding hydroperoxides isolated after hydrolysis proved to be very stable in the absence of iron.

[21] A. Bassan, M. R. A. Blomberg, P. E. M. Siegbahn, L. Que Jr, *Chem. Eur. J.* **2005**, *11*, 692–705.

[22] T. Ookubo, H. Sugimoto, T. Nagayama, H. Masuda, T. Sato, K. Tanaka, Y. Maeda, H. Okawa, Y. Hayashi, A. Uehara, M. Suzuki, *J. Am. Chem. Soc.* **1996**, *118*, 701–702; Y. Dong, S. Yan, V. G. Young, Jr., L. Que, Jr., *Angew. Chem.* **1996**, *108*, 673–676; *Angew. Chem. Int. Ed. Engl.* **1996**, *35*, 618–620; K. Kim, S. J. Lippard, *J. Am. Chem. Soc.* **1996**, *118*, 4914–4915; L. Que, Jr., *J. Chem. Soc. Dalton Trans.* **1997**, 3933–3940; A. L. Feig, S. J. Lippard, *Chem. Rev.* **1994**, *94*, 759–805; B. J. Waller, J. D. Lipscomb, *Chem. Rev.* **1996**, *96*, 2625–2657; J. T. Groves, *J. Inorg. Biochem.* **2006**, *100*, 434–447; J. M. Bollinger, Jr., C. Krebs, *J. Inorg. Biochem.* **2006**, 100, 586–605.

[23] There is growing evidence that $Fe^{IV}=O$ units take part in many oxidation reactions mediated by dinuclear iron compounds: D. Lee, S. J. Lippard, *Inorg. Chem.* **2002**, *41*, 827–837; F. Avenier, L Dubois, J.-M. Latour, *New J. Chem.* **2004**, *28*, 782–784; M. Kodera, M. Itoh, K. Kano, T. Funabiki, M. Reglier, *Angew. Chem.* **2005**, *117*, 7266–7268; *Angew. Chem. Int. Ed.* **2005**, *44*, 7104–7106; F. Avenier, L. Dubois, P. Dubourdeaux, J.-M. Latour, *Chem. Commun.* **2005**, 480–482; X. Shan, L. Que, Jr., *J. Inorg. Biochem.* **2006**, *100*, 421–433.

[24] Alternatively the formation of a Fe(μ-O)$_2$Fe diamond core structure[25] is conceivable but would not alter the discussion below significantly.

[25] L. Que, Jr., W. B. Tolman, *Angew. Chem.* **2002**, *114*, 1160; *Angew. Chem. Int. Ed.* **2002**, *41*. 1114–1137.

[26] Additionally, the data show that the alcohol functionality employed is always retained and thus not susceptible to attack by O_2 to yield the ketone.

[27] Compare for instance: P. Gosh, E. Bill, T. Weyhermüller, K Wieghardt, *J. Am. Chem. Soc.* **2003**, *125*; 3967–3979; S. Blanchard, E. Bill, T. Weyhermüller, K Wieghardt, *Inorg. Chem.* **2004**, *43*, 2324–2329; K. Cłopek, E. Bill T. Weyhermüller, K Wieghardt, *Inorg. Chem.* **2005**, *44*, 7087–7098; G. H. Spikes, E. Bill, T. Weyhermüller, K. Wieghardt, *Angew. Chem.* **2008**, *120*, 3015–3019; *Angew. Chem. Int. Ed.* **2008**, *47*, 2973–2977.

[28] M. E. Niño, S. A. Giraldo, E. A. Páez-Mozo, *J. Mol. Catal. A* **2001**, *175*, 139–151.

[29] SIR 2004: Program for Crystal Structure Determination, Perugia (Italy) **2005**; M. C. Burla, R. Caliandro, M. Camalli, B. Carrozzini, G. L. Cascarano, L. De Caro, C. Giacovazzo, G. Polidori, R. Spanga, *J. Appl. Crystallogr.* **2005**, *38*, 381–388.

[30] SHELXL-97, G. M. Sheldrick, Program for Crystal Structure Refinement, University of Göttingen, Göttingen (Germany) **1997**.

[31] K. S. Hagen, *Inorg. Chem.* **2000**, *39*, 5867–5869.

[32] R. A. Andersen, K. Faegri, Jr., J. C. Green, A. Haaland, M. F. Lappert, W.-P Leung, K. Rypdal, *Inorg. Chem.* **1988**, *27*, 1782–1786.

[33] J. S. Nowick, P. Ballester, F. Ebmeyer, J. Rebek, Jr., *J. Am. Chem. Soc.* **1990**, *112*, 8902–8906.